International Journal of Advanced Engineering Research and Science (IJAERS)
ISSN: 2349-6495(P) | 2456-1908(O)
Vol-8, Issue-2; Feb, 2021
Journal Home Page Available: https://ijaers.com/
Journal DOI: 10.22161/ijaers
Article DOI: https://dx.doi.org/10.22161/ijaers.82.38

Relationship between the Flooded Area and Cases of Malaria Disease before and after Construction of Jirau Hydroelectric Plant, Madeira River, Brazil

Johnatan Almeida de Sousa[1], Christiano Luna Arraes[2], Bruno Ferezim Morales[3]

[1]Distritio Sanitário Especial Indígena Alto Rio Negro. Avenidade 7 de Setembro, 500. São Gabriel da Cachoeira, AM - Brasil. CEP 69750-000. Email: eng.johnatanalmeida@gmail.com
[2] Instituto de Ciências Exatas e Tecnologia da Universidade Federal do Amazonas - ICET/UFAM. Rua Nossa Senhora do Rosário, 3863, Tiradentes, Itacoatiara, AM – Brasil, CEP.: 69103-128. Email: christianoarraes@yahoo.com.br
[3] Instituto de Ciências Exatas e Tecnologia da Universidade Federal do Amazonas - ICET/UFAM. Rua Nossa Senhora do Rosário, 3863, Tiradentes, Itacoatiara, AM – Brasil, CEP 69103-128/ Universidade Estadual Paulista "Júlio de Mesquita Filho". Instituto de Biociências, Programa de Pós-graduação em Ciências Biológicas, Rua. Prof. Dr. Antônio Celso Wagner Zanin, 250 - Distrito de Rubião Junior - Botucatu, SP - Brasil, CEP 18618-689, SP, Brasil.
Corresponding author: brunomorales@ufam.edu.br

Received: 02 Oct 2020;
Received in revised form:
16 Jan 2021;
Accepted: 11 Feb 2021;
Available online: 27 Feb 2021

***Keywords*—Landsat, Madeira River, Malária disease, Public health, Remote sensing.**

Abstract *- The operation of the Jirau hydroelectric plant, in the Madeira River near Porto Velho, Brazil started in 2013. Increased flooding areas near Jirau dam periodically reach communities with poor sanitation and can result in health problems, as the propagation of tropical diseases transmitted by aquatic vectors. Thus, we investigated the relationship between flooded areas and cases of malaria in Jirau´s Administrative Regions between 1994 and 2015. The flooded area was determined through spectral data (Landsat-5 and Landsat-8 satellite) and the numbers of malaria cases were extracted from the Epidemiological Surveillance Information System database of the Brazilian Ministry of Health. We verified an average flooded area of 770.3 km² before the dam (1994-2013) and 1370 km² after its operation (2014-2015). With linear regression between malaria cases and flooded areas, we verified a negative correlation during the study interval. Despite greater average flooded area after dam operation, the reduction of cases may be a result of several factors such as the imbalance of the parasitic relationship due to microclimatic changes, application of new substances for biological control (like artemisinin derivatives), little time for vector adaptation into new breeding sites, presence of plasmodium asymptomatic carriers, or even gaps or lack of case records in epidemiological databases. We highlight the importance of continuous monitoring of these variables and social control actions coverage expansion to prevent the risk of epidemic cycle occurrence and guarantee health security concerning this tropical disease and its socio-economic consequences.*

I. INTRODUCTION

The Madeira River is the main tributary of the Amazon River, with an extension of 1.238 km in Brazilian territory and an average flow of 23,000 m³ per second (Silva *et al.* 2013). It is formed by the rivers Guaporé, Mamoré and Beni, originated in the Andean highlands, and

its course is divided into lower and higher Madeira River (ANEEL, 2008).

The Jirau Hydroelectric plants on Madeira River started the operation in 2013, near the municipality of Porto Velho, north of Rondônia. The hydroelectric plant has an installed capacity of power generation around 3,300 MW, however, due to the operation with low water storage capacity in a very small reservoir, the effective production is around 2,184 MW on average (ONS, 2019).

Hydroelectric plants along the Madeira river increased potential risks and vulnerabilities in the Porto Velho region, Rondonia state, Brazil. Among these, we highlight changes in population and socio-economic profile, hydrological cycle, environmental characteristics, biological relationships, and ecological processes (Rodrigues *et al.* 2019).

Another problem is the formation of flooded areas and changes in the natural flooding process. This results in the displacement of the resident population in the area that will be flooded by the reservoir and, consequently land losses. Flooded areas are relevant to health due to their intrinsical relationship with some infectious diseases of water transmission, like malaria. So the extent of flooded areas determines the potential presence of sites for the proliferation of insects and vectors of these diseases.

Several studies had developed methodologies for monitoring flooded areas (Baldassarre, 2009); (Asadzadeh, 2013), mainly through remote sensing techniques, using satellite images that represent important tools for mapping temporal modeling of flood areas (Wardah, 2008; Baki and Gan, 2012;Villar, 2013).

Considering the multiple ecosystem services provided by Amazon ecosystems, the construction of dams cannot be dissociated from studies of its impacts in all knowledge fields, which also includes the possible effects of floods in their coverage areas and its potential influence on public health.

In this context, to understand the processes arising after the installation of the Jirau dam, this study focused on remote sensing as a tool to investigate changes in habitats e and verify the association of water coverage (flooded area) with the number of cases of waterborne diseases, with an emphasis on malaria. Therefore, we traced the temporal water coverage profile of Jirau dam before, during, and after the construction of the hydroelectric plant, located in the coordinates: 9° 15' 52"S and 64° 38' 31"W and obtained the number of infections for each year

This paper addressed the main aspects of the literature of remote sensing as a monitoring tool, impacts of dams on the landscape, and potential relationships between floods and health aspects. Methodological procedures included study area description, steps of geoprocessing for flooded area coverage estimation, acquisition of malaria records in government databases, and linear regression between flooded area and numbers of malaria cases.

II. METHODS

2.1 Study area

The Jirau Hydroelectric Plant, located on Madeira River, is entirely inserted in the municipality of Porto Velho, State of Rondônia, Brazil (Figure 1). Jirau dam is located on Jirau rapids, immediately downstream of Inferno waterfalls and about 130 km upstream of the city of Porto Velho (Costa, 2013). The formed reservoir has an area of 361.6 km2. The flooding area varies between 21 km2 and 207.7 km2 at the geographical coordinates 9° 15' 52"S and 64° 38' 31"Q (Rodrigues, 2019).

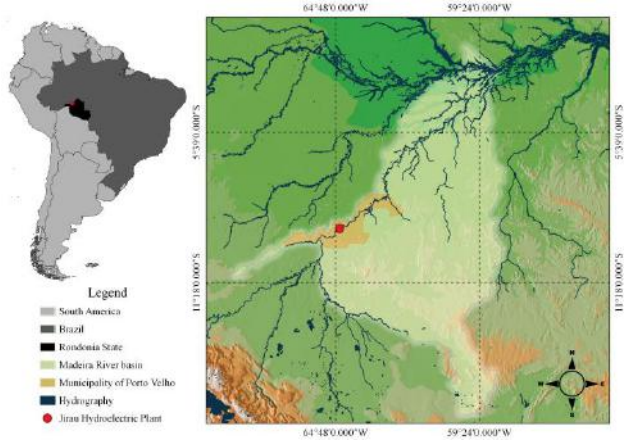

Fig.1: Map of study area showing the location of Porto Velho and areas under the influence of the Jirau Hydroelectric Plant, Rondônia State, Brazil.

2.2 Geoprocessing techniques

Spectral data used in this study were obtained from the Thematic Mapper (TM) sensor of Landsat-5 satellite and Operational Land Imager (OLI) sensor of Landsat-8 satellite. The imagery collection was acquired from the database of the Brazilian National Institute for Space Research (INPE). To calculate the reflectance values of the Earth's surface, scenes 232/66 and 233/66 with a bandwidth of 760 to 900 nm from the years 1994 to July 2015 (Table 1) were manipulated with ENVI software (ENVI, 2005). These scenes have a spatial resolution of 30m and a 16-day temporal resolution.), for both sensors. The bandwidth corresponds to the region of the near-infrared, where water bodies are reflected as dark (i.e.

black) and the vegetation reflection is white (Nascimento*et al.*2014)

Table 1: Date reference of Spectral data of Thematic Mapper Sensor (TM) and Operational Land Imager (OLI)

Orbit/ Point	Thematic Mapper (TM)	Operational Land Imager (OLI)
232/66	Date	Date
	07-08-1994	08-06-2013
	01-07-1998	11-06-2014
	06-07-2000	
	02-06-2005	13-07-2014
	28-07-2007	14-06-2015
	04-06-2009	16-07-2015
	13-08-2011	
233/66	Date	Date
	27-06-1994	01-07-2013
	08-07-1998	02-06-2014
	11-06-2000	
	11-07-2005	14-07-2014
	28-07-2007	
	04-06-2009	05-06-2015
	13-08-2011	07-07-2015

The Jirau reservoir is inserted in two tiles (232/66 and 233/6), so it was necessary to create a mosaic with these images. Images obtained from the TM sensor-Landsat 5 were georeferenced because they don't have a cartographic reference system. Georeferencing process consists of a set of numerical operations that modify or alter its geometry to adjust it to a coordinate system considered as a reference (Weber, 2006).

To perform this procedure, a polynomial equation was used, whose coefficients were calculated from control points. These points were identified in the image to be adjusted and in the desired reference system, and a uniform spatial distribution should be found (Richards, 1995; Mather, 1999). The equation establishes a relationship between the coordinates of the image (line, column) and the defined cartographic reference system. After applying the polynomial function to transform the geometry of an image into a plane and/or geographic coordinate system, errors are generated (Equation 1), where EMQ is the mean square error; pt is the difference between the positions (x and y) of the reference control point of the point in the image after the transformation; and subscripts 1, 2 ... n denote control points.

$$EMQ = \sqrt{\frac{pt_1^2+pt_2^2+pt_{2n}^2}{n}} \quad (1)$$

In the ENVI software (ENVI, 2005) the RMS value, after making 60 control points, must have a maximum of between 0.8 and 0.9 (Weber, 2006), in units of pixels. When the geometric corrections of the images were obtained based on a georeferenced product, different compositions were made with three-band arrangements, in the following sequences: True color R3G2B1, False color R4G3B2, False natural color R5G4B3 (Rosa *et al.* 2011). For the TM sensor images, the false natural color R5G4B3 was chosen because it makes a better distinction between the targets of interest, while for the OLI images the color composition R5G6B4 was chosen, which makes the best distinction between soil and water (Butler, 2013).

2.3 Flooded area coverage estimation

The coverage of flood area was estimated through the Normalized DifferenceVegetation Index (NDVI), which considers the transformation of the reflectance from the TIFF images obtained from the satellite sensors. However, before reaching the reflectance result, is necessary to obtain the terrestrial latitude angle (Φ), where the minutes of degree were converted into decimal fractions of a degree, the hour angle (ω), which is an angular deviation value whose value is null when the local time is half a day, considering that the Earth rotates 15 ° every hour (Campos, 2013). The hour angle is expressed in Equation 2, where T is the solar time h in the considered place and T varies between 0 and 24 hrs.

$$\omega = (12 - T) * 15 \quad (2)$$

According to Campos (2013), there is a seasonal variation of the terrestrial axis inclination of 23º 27' to the normal on the ecliptic plane. The solar declination perceived by an observer at the terrestrial equator, on a given day of the year (J), is given by Equation 3, where is the solar declination value in degrees, and J indicates the order number of Julian days.

$$\delta = 23{,}45°.sen\left[\frac{360*J-80}{365}\right] \quad (3)$$

After obtaining the declination values, we calculated the solar altitude, which is the angle between the direction of the radiation and the projection of this same direction in the horizontal plane. For this, the Equation 4, proposed by Messenger (2010) was used (where α (alpha) is the value of the angle of the solar altitude, given in degrees and is the angle of the terrestrial latitude);

$$\alpha = sen^{-1}(sen\delta.sen\Phi + cos\delta.cos\Phi.cos\omega) \quad (4)$$

The additional steps were to calculate the radiance and the reflectance (Equation 6) for bands 3 and 4 of Landsat 5 / TM. This allowed the conversion of Digital Numbers (DN) into monochromatic reflectance effectively (Neto et al., 2008). For the Landsat 5/TM images, there is a (DN) min and (DN) max of 0 and 255 respectively, since the radiometric resolution is 8 bits. while for Landsat-8/OLI images, the range of (DN) value is between 0 to 65535, since the images have a 16-bit radiometric resolution (Neto et al., 2008).

To calculate radiance (Equation 5), DN is the Digital number of each pixel; (DN) min and (DN) max are the Minimum and maximum value that DN can reach; L min L L max area the Calibration constants for a given sensor; Lλ is Monochromatic spectral radiance (W⁄m.sr.µm).

$$L_\lambda = \left(\frac{L_{máx}-L_{mín}}{DN_{máx}}\right) x(DN) + L_{mín} \quad (5)$$

The monochrome reflectance was obtained with Equation 6, where dr = Inverse of the square of the Earth-Sun distance in astronomical units; z = Zenith solar angle (degrees) at the time of acquisition; Eλ = Average solar irradiance at the top of the atmosphere (mW⁄(cm².Ω.µm));Lλ = Monochromatic spectral radiance (W⁄m.sr.µm); ρλ = Monochromatic reflectance) by:

$$\rho_\lambda = \frac{\pi.L_\lambda}{E_\lambda.cos(z).d_r} \quad (6)$$

We obtained the equation for direct conversion (Equation 7) of the digital number into reflectance substituting Equation 5 in Equation 6.

$$\rho_\lambda = \frac{\pi.\left[\left(\frac{L_{máx}-L_{mín}}{DN_{máx}}\right)x(DN)+L_{mín}\right]}{E_\lambda.cos(z).d_r} \quad (7)$$

After determining the physical values of reflectance of the images, the NDVI was calculated, which according to Rosemback et al. (2005) is given by Equation 8, where ρivp = reflectance value in the near-infrared range; ρv = Value of reflectance in the red band.

$$NDVI = \left(\frac{\rho_{ivp}-\rho_v}{\rho_{ivp}+\rho_v}\right) \quad (8)$$

The NDVI valuesobtained are contained in a scale that ranges from values between -1 to 1 (Neto *et al.* 2008). The delimitation of the flooded surfaces was carried out as described by Sakamoto (2010), which consists of three phases: (i) composition of the bands derived from the calculation of the NDVI, (ii) comparison of these indices to identify and separate the different classes of land use, (iii) generation of classified images for the entire time series, delimiting the water bodies of other land uses. The last phase was defined by four distinct classes: free water (totally floodable regions), floodable vegetation (temporarily flooded regions), non-floodable vegetation (regions covered with vegetation without flooding), and other regions that are not of interest in this study (Santos, 2009). To calculate the areas flooded by the hydroelectric dam, the software Envi 4.5 and Qgis were used to obtain the results of the area flooded in km².

2.4 Acquisition of malaria cases

Data of registered cases of malaria in the studied area were collected from the Ministry of Health, Health Surveillance Secretariat (SVS), Epidemiological Surveillance Information System, and demographic databases from the Brazilian Institute of Geography and Statistics (IBGE). The malaria disease data extracted from the Epidemiological Surveillance Information System - Malaria (SIVEP-Malaria) was from 2004 to 2016.

To verify the relationship between the flooded surface area and the cases of malaria in the entire construction process (beforeand after) the Jirau hydroelectric plant, we followed the work of Viana (2003) who treats this relationship as the main aspect to cause environmental changes and social disruptions. According to this author, big dams generate serious problems for the health of the affected population.

Malaria disease was represented in the analysis by the Annual Parasitic Index (IPA), which has the number of positive malaria tests (codes B50 to B53) per thousand inhabitants, in a given geographical space, in the year considered (RIPSA, 2017).

The risk of the occurrence of malaria was estimated in the population in the region of influence of the Jirau reservoir during period selected for this study, and the respective population exposed to the risk of acquiring the disease.

In Brazil, endemic areas are located in the Legal Amazon Region, with degrees of risk expressed in IPA values ranging from low (0.1 to 9.9), medium (10.0 to 49.9), and high (greater or equal to 50.0).

The use of malaria IPA makes it possible to assess the risk of malaria transmission in a given geographical space, to analyze population, geographic and temporal variations in the distribution of malaria cases. This represents an important piece of the set of epidemiological and environmental surveillance actions for malaria and alsocontributes tosubsidize planning, management, and

evaluation processes of health policies and actions aimed at controlling vector-borne diseases (DATASUS, 2010). The method of calculating the malaria IPA can be expressed in Equation 9, where NPE = number of positive malaria tests; PR = resident population in a given region and time.

$$IPA = 1000x\frac{NPE}{PR} \quad (9)$$

2.5. Relationship between flooded area and health aspects

The relationship between flooded areas and IPA (i.e. health aspects) was verified with linear regression. According to Peternelli (2002), this analysis makes it possible to verify the correlation between two distinct quantitative variables.

III. RESULTS AND DISCUSSION

NDVI values were calculated for all years under study based on data of TM sensor and OLI sensor in a 2-year interval from 1994 to 2015. However, in 2013, the year that the OLI sensor and Jirau Hydroelectric Plant started operation, satellite images were entirely covered by clouds, interfering in the accuracy of the estimation of the flooded surface. To compensate this, NDVI was calculated for the June and July of the years 2014 and 2015.

The values of 1994, 1998, 2000, 2005, 2007, and 2009 were before any intervention on the Madeira River channel in the current location of Jirau reservoir. In 2011 part of the dam was already installed and the course of the Madeira River was deviated, during the construction period. In 2013, the Hydroelectric Plant started operation. The years 2014 and 2015 represented the period after the installation of the dam.

We observed a remarkable increase in flooded areas upstream and downstream of the Jirau dam (Table 2). The average flooded area before the dam, calculated between 1994 and 2009, was 770.3 km², while in 2011 this area increased to more than 867.3 km², and continuously increased after 2013, reaching 335.2 km² in July 2015. According to the inspection report of the Federal Secretariat of Internal Control, Porto Velho - RO (CGU, 2014) the area under influence of the Jirau reservoir was affected in its physical, environmental, and economic aspects.

This scenario was the result of the elevation of the Madeira River up to the historical quota of 19.74 m on March 30, 2014, a measure that corresponds to 3.06 m above the value already considered as overflow quota. We highlight that the quotas registered in the higher historical floods were 17.44 m and 17.50 m in 1984 and 1997 respectively). After the operation of the Jirau Hydroelectric Plant, the most critical level of the flooded area was in 2015.

Table 2: Flooded surface in areas under influence of Jirau Hydroelectric Plant, in Porto Velho, State of Rondonia, Brazil, between 1994 and 2015.

Years	Flooded area(Km²)
1994	747.6147
1998	729.6669
2000	778.3920
2005	831.0465
2007	763.6455
2009	771.4989
2011	867.3948
June 2014	1,335.2877
July 2014	1,319.4351
June 2015	1,376.8002
July 2015	1,370.3085

The influence of the Jirau dam in increasing the flooded area of surrounding territories has the potential to result in socio-environmental and ecological impacts such as habitat fragmentation, native fauna and flora loss, and relocation of residents, mainly upstream of the dam. As more water is available in inhabited areas, the possibility of insect vectors for diseases such as malaria increases.

Porto Velho represented 64.8% of the registered cases of malaria disease in 2014 (BRASIL, 2017), considering all Administrative Regions of Rondônia State. According the Rondonia's State Program for Malaria Control (PECM/AGEVISA-RO, 2017), the municipalities of Alto Paraíso, Candeias do Jamari, Cujubim, Guajará-Mirim, Itapuã do Oeste, Machadinho do Oeste and Porto Velho are in the transmission area of malaria, while Castanheiras, Cerejeiras, Chupinguaia, Colorado do Oeste, Corumbiara, Espigão do Oeste, Minister Mário Andreazza, Mirante da Serra, Novo Horizonte, Nova União, Parecis, Presidente Médici, Primavera de Rondônia, Santa Luzia do

Oeste, São Felipe do Oeste and Vilhena were free of the disease.

Based on the database obtained for governmental sources, we verified that the number of cases of malaria in Porto Velho has substantially decreased between the years evaluated in this study (Table 3).

Table 3. Number of registered cases of malaria disease in Porto Velho, State of Rondonia, Brazil, between 2004 and 2016.

Years	Number of cases (malaria)
2004	33,942
2005	44,464
2006	36,108
2007	32,774
2008	21,994
2009	19,766
2010	22,887
2011	18,247
2012	16,953
2013	8,221
2014	6,409
2015	2,965
2016	1,782

The decreasing behavior observed in Porto Velho, a region under influence of the Jirau reservoir, is in line with the report of the World Health Organization (WHO), which describes that malaria has been showing a reduction in its incidence in all countries, since it went from approximately 500 million cases in 2010 to 198 million cases in 2013, that represents a reduction of 60.4% (WHO, 2015). According to Brazil (2015), in the same period mentioned in the WHO report, Porto Velho presented a 64.1% reduction in the number of malaria cases.

The reduction in the number of malaria cases over the years may have been influenced by climate changes, considering that these changes can modify the conditions of disease transmission (Kovats, 2000). In Porto Velho, another potential factor may be the introduction of a new drug combined with artemisinin derivatives to control the malaria disease vector (BRASIL, 2006).

The linear regression between the number of malaria cases and the flooded area indicated a negative correlation between these variables ($R^2 = 0.5369$, Slope = -18.80 and $p < 0.05$; Figure 2) which leads to the inference that the number of malaria cases in Porto Velho decreased in the years evaluated while the flooded area increased.

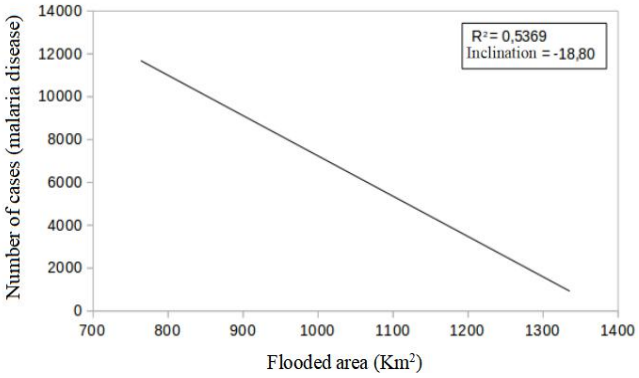

Fig.2: Linear regression between the number of malaria cases and the flooded area in Porto Velho, Rondonia State, Brazil, between 2004 and 2015.

Anopheles darlingi, the main vector of malaria in Amazonian environments shows, in the northern region, greater abundance in anthropized environments (Oliveira and Luz, 1996). Previous studies also carried out in the North region, notably in the state of Rondônia, also demonstrated the synanthropy of these vectors (Klein and Lima, 1990). According to the data analyzed, it can be seen that there has been a significant increase in the population in all ARs since 2010, but the same has not happened with malaria cases, given that there was a decline in all regions during the year. analyzed period.

For malaria disease, in the case of the construction of dams, the number of breeding areas of the vector mosquito may increase and contact with people may be intensified, so there is an expected increase in the risk of infestation and consequently in the number of cases (Tubaki *et al.* 2004).

Lima (2016) raises the possibility that the filling of the Jirau reservoir may have eliminated numerous breeding sites, given the increase in the water mirror, however, the possibility of forming others is not extinguished, as the adaptation of the vector to these new breeding sites is just a matter of time (Lima, 2016). Considering that the presence of asymptomatic patients with plasmodium (Camargo *et al.* 1999; Alves*et al.* 2002;

Lima, 2016), plus the presence of vectors, the risk of future epidemic cycles cannot be overlooked.

Our results show that, in absolute numbers, malaria showed a sharp decline, even with the increase in the flooded area in the area influenced by Jirau reservoir. However, Lima (2016) registered an increase in the detection of malaria disease by *Plasmodium falciparum* (which causes 90% of malaria cases) in the same period in the region studied. So this scenario can be represent a period of adaptation of the vector to the new landscape scenario and ecological patterns, efficiency of the vector control with combined drugs, or deficiency in the system of registration and identification of the cases of malaria in the region by the health and epidemiological service at the local, regional and state levels.

We emphasize that more flooded areas together with the presence of vectors can represent optimal conditions to malaria diseases and the risk of future epidemic cycles cannot be overlooked and must be treated as a priority in public policies.

IV. CONCLUSIONS

In the years 1994 to 2009, there was no substantial change in the flooded area when compared to the years to the increase verified for 2011, 2014, and 2015.

The average flooded area from 1994 to 2009 was 770.3 km². After installing part of the dam in 2011, this area increased to more than 867 km², in the period of June 2014 and July 2014 this flooded area increased to more than 1318 km² and for the same period of 2015, this flooded area increased to more than 1370 km².

Remote sensing techniques can be used for temporal analysis, as well as monitoring flooded areas.It was expected that the incidence of disease would be entirely linked to the increase in the flooded area due to the displacement of workers to the region, however, a negative relationship was found. The linear regression model indicated that the number of cases of malaria decreases with the increase in the flooded area.

Although the data show a decline in the number of malaria cases in the years studied, there is a need to continue the present study to verify whether this correlation can become positive, since due to the adaptation of the vector, it may be that in the course of years there has been an increase in malaria epidemic cycles.

ACKNOWLEDGMENTS

We are grateful to Instituto de Ciências Exatas e Tecnologia of Universidade Federal do Amazonas for computational equipment allowance to perform the spatial data analysis. We are in debt to Instituto Nacional de Pesquisas Espaciais - INPE, Ministério da Saúde do Brasil, Secretaria de Vigilância em Saúde (SVS), Sistema de Informações de Vigilância Epidemiológica for data availability.

REFERENCES

[1] ANEEL. Agência Nacional de Energia Elétrica. (2008) Leilão UHE Jirau. Complexo Hidrelétrico do Rio Madeira. 4 p.

[2] Asadzadeh, A. et al. Evaluation of multiple satellite altimetry data for studying inland water bodies and river floods. Journal of Hydrology, v. 505, p. 78–90, 2013.

[3] Baki, A.B.M., Gan, T.Y. (2012). Riverbank migration and island dynamics of the braided Jamuna River of the Ganges and Brahmaputra basin using multi-temporal Landsat images. Quaternary International, 263: 148–161.

[4] Baldassarre, G.D., Schumann, G., Bates, P. D. (2009). A technique for the calibration of hydraulic models using uncertain satellite observations of flood extent. Journal of Hydrology, 367(3-4): 276–282.

[5] Basahi, I. A. (2000). Marib Dam: the importance of environmental and health impact studies for development projects. Eastern Mediterranean Health Journal, 6 (1): 106 - 117.

[6] Bermanm, C.A. (2002). Perspectiva da Sociedade Brasileira Sobre a Definição e Implementação de Uma Política Energética Sustentável – Uma Avaliação da Política Oficial. Projeto Brasil Sustentável e Democrático.

[7] BRASIL, Ministério da Saúde. (2017). Sistema de Informação de Vigilância Epidemiológica. SIVEP – Malária. Retrieved from http://www.saude.gov.br/sivepmalaria

[8] BRASIL. Ministério da Saúde. (2006). Ações de Controle da Malária. Manual para Profissionais de Saúde na Atenção Básica. Série A. Normas e Manuais Técnicos. 1ª ed. Brasília.

[9] Butler, K. (2016) Band Combinations for Landsat 8. Retrieved from https://blogs.esri.com/esri/arcgis/2013/07/24/band-combinations-for-landsat-8/

[10] Campos, M.S. (2013). Programa Para o Cálculo da Variação da Direção de Incidência dos Raios Solares ao Longo Do Ano. COBENGE.

[11] Chavez Jr., P.S. (1998). An improved dark-object subtraction technique for atmospheric scattering correction of multispectral data. Remote Sensing of Environment, (24): 459-479.

[12] Confalonieri, U.E.C. (2005). Saúde na Amazônia: um modelo conceitual para a análise de paisagens e doenças. Estudos Avançados.

[13] CGU - CONTROLADORIA GERAL DA UNIÃO. (2014). Secretaria Federal de Controle Interno. Relatório de Fiscalização nº 201408699. Diagnóstico Situacional dos Efeitos da Cheia do Rio Madeira em Porto Velho, Rondônia. Relatório..

[14] Costa, F. (2009). Relatório Técnico sobre a malária no município de Porto Velho, período de 01 a 30 de setembro. Programa de Saúde Pública, Sub-Programa de Vigilância Epidemiológica. Energia Sustentável do Brasil.

[15] Costa, P. (2013). UHE jirau entra em operação comercial. Newsletter CBDB.

[16] Costa, R.H. (2011). Desterritorialização: entre as redes e os aglomerados de exclusão. In: CASTRO, Iná Elias de; GOMES, Paulo César da Costa; CORRÊA, Roberto Lobato. (Org.). Geografia: conceitos e temas. 14.ed. Rio de Janeiro: Bertrand Brasil, .

[17] Couto, R.C.S. (1996). Hidrelétricas e saúde na Amazônia: um estudo sobre a tendência da malária na área do lago da hidrelétrica Tucuruí. Escola Nacional de Saúde – FIOCRUZ. p.135.

[18] Cureau, S. (2014). Os Impactos Socioculturais Decorrentes da Construção de Usinas Hidrelétricas no Brasil.

[19] DATASUS. (2017). Índice Parasitário Anual (IPA) de malária – D.4. 2010. from http://tabnet.datasus.gov.br/tabdata/LivroIDB/2edrev/d04.pdf.

[20] ENVI (2005). Envi user's guide, The Environment for Visualizing Images. Version 4.2. Colorado, U.S.A. CD-ROM.

[21] Freitas, C.M., Ximenes, E.F. (2012). Enchentes e saúde pública: uma questão na literatura científica recente das causas, consequências e respostas para prevenção e mitigação. Ciência & Saúde Coletiva.

[22] Goitia, P.S.D. et al. (2016). A expansão das usinas hidrelétricas na região amazônica: desafios operacionais e regulatórios. Congresso Brasileiro de Planejamento Energético. Gramado-RS.

[23] Harinasuta, C., Jetanasen, S., Impand, P., Maegraith, B.G. (1970). Health problems and socioeconomic development: investigation on the pattern of endemicity of the diseases occurring following the construction of dams in northeast Thailand. Southeast Asian Journal of Tropical Medicine and Public Health. (4): 530 - 552.

[24] Katsuragawa, T.H. (2006). Prevalência de algumas doenças em população residente em áreas de influência de Usinas Hidrelétricas, no município de Porto Velho, Amazônia Ocidental. Porto Velho: Universidade Federal de Rondônia.

[25] Kovats, R.S. (2000). El Niño and human health. Bull WHO. 78(9):1127-35.

[26] Lima, A.A. (2016). Malária no município de Porto Velho: análise espacial dos casos de incidência no período de 2004 a 2014. Dissertação de Mestrado em Biologia Experimental. Universidade Federal de Rondônia. Porto Velho. 91 p.

[27] Manyari, W.V. (2007). Impactos Ambientais a Jusante de Hidrelétricas, o Caso da Usina de Tucuruí, PA. Universidade Federal do Rio de Janeiro.

[28] Mather, P.M. (1999). Computer processing of remotely-sensed images: an introdution. 2 ed. p.292.

[29] Messenger, R.A., Ventre J. (2010). Photovoltaic systems engineering. CRC Press LLC, 3.ed, cap. 2, p 21-46.

[30] Nascimento, S., Lima, E., Lima P. (2014). Uso do NDVI na Análise Temporal da Degradação da Caatinga na Sub-Bacia do Alto Paraíba. Revista OKAPA: Geografia debate; 8(1): 72-93.

[31] Neto, L.F., Bertoni, J. (2008). Conservação do solo. 6ed. p.355.

[32] Neto, R. et al. (2008). Determinação de Valores Físicos De Imagens Tm/Landsat- 5 Utilizando A Linguagem Legal Para Obter Índices De Vegetação. II Simpósio Brasileiro de Ciências Geodésicas e Tecnologias da Geoinformação. Recife – PE, 8-11.

[33] Oliveira, K. (2012). Porto Velho e as Usinas Hidrelétricas de Santo Antônio e Jirau: Riscos e Vulnerabilidades Socioambientais. Revista Geonorte, Edição Especial 2, 2(5): 565-572.

[34] ORGANIZAÇÃO MUNDIAL DE SAÚDE – OMS. (2015). Relatório Mundial da Malária.

[35] PECM/AGEVISA-RO. PROGRAMA ESTADUAL DE CONTROLE DA MALÁRIA –AGÊNCIA ESTADUAL DE VIGILÂNCIA EM SAÚDE DE RONDÔNIA. (2017). Controle de Malária. Retrieved from http://www.rondonia.ro.gov.br/agevisa/institucional/vigilancia-ambiental/controle-de-malaria/

[36] Peteternelli, L.A. (2002). Regressão Linear e Correlação. INF 192.

[37] Richards, J.A. (1995). Remote Sensoring Digital Image Analysis. Springer-Verlag.

[38] RIPSA – Rede Interagencial de Informações Para a Saúde. (2017). Índice Parasitário Anual (IPA) de malária. Indicador: D.4. 201-. Retrieved from http://www.ripsa.org.br/fichasIDB/pdf/ficha_D.4.pdf

[39] Rodrigues, L.A.L. (2019). Licenciamento ambiental em números: uma comparação entre as uhes santo antônio, jirau e belo monte. Dissertação de Mestrado. Proograma de Pós-graduação em Planejamento Energético, COPPE, Universidade Federal do Rio de Janeiro, UFRJ.

[40] Rosa, L., Alves, M.C., Sanches, L. (2011). Uso de Composição de Bandas do Satélite Landsat 5 TM para Caracterizar a Dinâmica da Variação de Áreas Alagadas no Pantanal Mato-Grossense. INPE. p. 5992-5999.

[41] Rosemback, R., França, A.M.S., Florenzano, T.G. (2005). Análise comparativa dos dados NDVI obtidos de imagens CCD/CBERS-2 e TM/LANDSAT-5 em área urbana. Anais XII SimpósioBrasileiro de SensoriamentoRemoto, Goiânia, Brasil.

[42] Sakamoto, T. et al. (2010). A Two-Step Filtering approach for detecting maize and soybean phenology with time-series MODIS data. Remote Sensing of Environment, 114(10): 2146-2159.

[43] Santos, J. et al. (2009). Dinâmica de inundação em zonas úmidas da bacia amazônica por meio de dados espaciais. Associação Brasileira de Recursos Hídricos. p. 1–16.

[44] Saraiva, M.G.G. et al. (2009). Expansão urbana e distribuição espacial da malária no município de Manaus, Estado do Amazonas.
[45] Silva, L., Filizola, N., Souza, C. (2013). Análise Multitemporal da Variabilidade de Cotas Fluviométricas do Rio Madeira – Uma Avaliação de Danos Sob Extermas Condições Hidrológicas – Brasil. SBSR. XVI Simpósio Brasileiro de Sensoriamento Remoto. Foz do Iguaçu: INPE.
[46] Sow, S., De Vlas, S.J., Engels, D., Gryseels, B. (2002). Water-related disease patterns before and after the construction of the Diama dam in northern Senegal. Annals of Tropical Medicine and Parasitology, 96 (6) 575 - 586.
[47] Stolerman, P. et al. (2014). A implantação da Usina Hidrelétrica de Jirau no rio Madeira e os processos de desterritorialização em Rondônia. Terra Plural.
[48] Tundisi, J. G. (2007). Exploração do potencial hidrelétrico da Amazônia. Universidade de São Paulo, 21(59): 109 – 117.
[49] Viali, L. (2008). Testes de Hipóteses não Paramétricos. Instituto de Matemática – Departamento de Estatística. Porto Alegre.
[50] Viana, R.M. (2003). Grandes barragens, impactos e reparações: um estudo de caso sobre a barragem de Itá. RJ, Dissertação de Mestrado, IPPUR/UFRJ, Rio de Janeiro.
[51] Villar, E.R. et al. (2013). A study of sediment transport in the Madeira River , Brazil , using MODIS remote-sensing images. Journal of South American Earth Sciences, 44: 45–54.
[52] Wardah, T. et al. (2008). Use of geostationary meteorological satellite images in convective rain estimation for flash-flood forecasting. Journal of Hydrology, v. 356, n. 3-4, p. 283–298.
[53] Weber, E. (2006). Tarefas e Produtos Desenvolvidos. UFRGS.